ELSEVIER

Effects of cooling rate on fracture resistance of nylon 6-silicate nanocomposites

Savas Avlar, Yu Qiao*

Department of Civil Engineering, University of Akron, Akron, OH 44325-3905, USA

Abstract

In this paper, the fracture resistance of nylon 6-silicate nanocomposites was measured as function of silicate content and cooling rate. The addition of silicate nanolayers resulted in a significant decrease in toughness in air cooled samples. In cold water quenched samples, however, the total fracture work was comparable with that of neat nylon 6, providing a promising way for the simultaneous enhancement of stiffness, strength, and toughness. The effect of cooling rate on the semi-crystalline matrix structure and its role in fracture behavior were discussed.
© 2004 Elsevier Ltd. All rights reserved.

Keywords: A. Nano-structures; A. Polymer–matrix composites (PMCs); B. Fracture toughness; E. Cure

1. Introduction

Reinforcing thermoplastics, including nylon 6, with silicate nanolayers has been an active research area for the past decade (e.g. [1]). A number of experimental processing development studies have explored the disruption and dispersion of the silicate platelets [2,3]. In addition, certain design strategies have been developed for optimizing design variables [4,5]. Various experimental results have showed that with a relatively low silicate content in the range of 1–5 wt%, the stiffness and strength can be improved significantly. As a 'side effect', the ductility is usually lowered [6,7], indicating clearly that the strength enhancement is mostly achieved through the suppression of plastic deformation. Because of the lack of the ability to deform plastically, the elastic domain expands and thus the yield strength increases. However, if defects exist, the extent of energy dissipation of plastic deformation in the near-tip field is reduced, leading to the high level of brittleness.

The reason why the silicate nanolayers tend to lower the ductility is still inadequately understood. It is not clear (1) how the silicate nanolayers influence the morphology of the semi-crystalline matrix under various processing conditions, and (2) whether this is a more important factor than the silicate–matrix interaction itself, especially under the plane strain condition at the crack tip. On the one hand, the presence of silicate nanolayers can decrease the mobility of amorphous chains and increase the number of nucleation sites, which results in a fine semi-crystalline structure and relatively high tie-molecule density. On the other hand, the craze density is reduced considerably and the craze propagation can be difficult.

In addition to the degree of exfoliation of silicate nanolayers, another important design variable affecting the matrix morphology and the filler–matrix interaction is the cooling rate. In slowly cooled nylon 6-silicate nanocomposites, the α form is important when the silicate content is low. With the addition of nanofillers, the formation of the γ form is promoted due to fine-scale heterogeneous nucleation [8]. As the cooling rate increases, this effect becomes increasingly pronounced and eventually the γ form is dominant. With the high cooling rate, the peak crystallization temperature is low, since the degree of undercooling rises as the characteristic crystallization time decreases [9]. Unlike in neat nylon 6, the crystallinity in nanocomposites can increase with cooling rate, which was attributed to the high crystallization rate of the γ form [10]. Note that the activation energy is independent of the silicate content [11].

* Corresponding author. Tel.: +1 330 972 2426; fax: +1 330 972 6020.
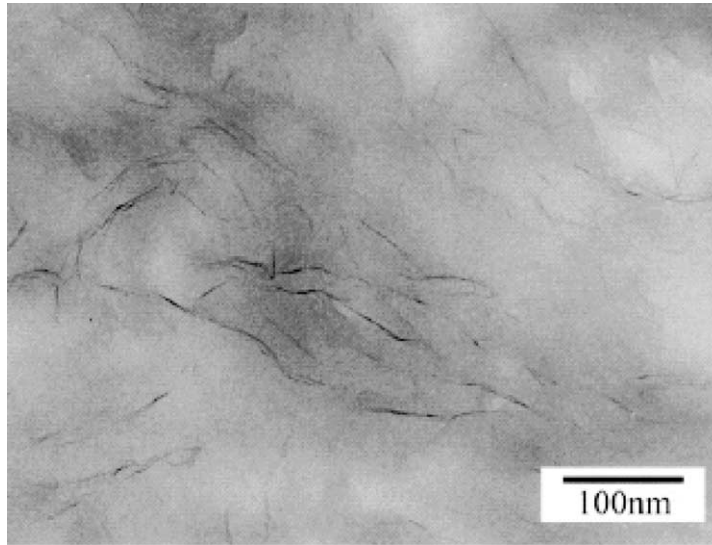*E-mail address:* yqiao@uakron.edu (Y. Qiao).

Fig. 1. TEM microscopy of a thin section of the nylon 6-silicate nanocomposite [12].

In view of the above considerations, in this paper we carried out experimental studies on the fracture resistance of nylon 6-silicate nanocomposites of various silicate contents prepared through different cooling procedures. It was found that increasing cooling rate has little influence on the toughness of neat nylon 6, but is beneficial to the nanocomposites.

2. Experimental

2.1. Material preparation

The nylon 6-silicate nanocomposites studied in this paper were provided by Dr M. Kato in the Toyota CRD Lab, Inc. By displacing the ions in the interlayer of Na-montmorrillonite followed by an in situ polymerization process, silicate layers were exfoliated into and well mixed with the nylon 6 matrix (see Fig. 1) [12–14]. After rinsing and drying, the master batch was cooled down and cut into pellets. In samples formed through injection molding, there exist strong orientational and positional correlations among the nanolayers [15], while compression molding usually leads to an isotropic structure [3].

Materials with three different silicate contents, N-6, NS-17, and NS-37, have been tested. N-6 is neat nylon 6 and the other two are nanocomposites of the silicate contents of 1.7 and 3.7 wt%, respectively. The weight density of the nylon 6 matrix is 1.1×10^3 kg/m^3 and that of the silicate nanolayers is 2.4×10^3 kg/m^3. After drying at 80 °C for 24 h in a type 285 A Isotemp vacuum oven, the pellets were hot pressed into thin plates at 240 °C in air under 2.1 MPa in a type 3912 Carver hydraulic compression molding machine. The high temperature was maintained for about 8 min to minimize the influence of heat treatment history. Then, the plates were either air cooled with the mold or cold

water quenched. The cooling rates were about 5 °C/min and 100 °C/s, respectively. The mold was made from 304 stainless steel with the size around $200 \times 200 \times 50$ mm. The plate thickness, B, was about 0.5 mm. The tensile modulus, tensile strength, and ductility were measured in tensile experiments at room temperature and the results are listed in Table 1. It can be seen that the tensile modulus and strength are insensitive to the change in cooling rate.

2.2. Fracture experiment

The plate samples with the length, L, of 50 mm and the width, W, of 4.8 mm were cut from the thin plates using a precision-positioning steel stage. The precracks were produced by a razor blade. The radius of the crack tip was less than 0.1 mm. The precrack length, a_0, was 1.2 mm. The fracture experiments were performed at room temperature in a type 5569 tabletop Instron machine in displacement control mode, with the crosshead speed of 1.0 mm/min.

Table 1
The mechanical properties of the nylon 6-silicate nanocomposites

	N-6		NS-17		NS-37	
	Air cooled	Cold water quenched	Air cooled	Cold water quenched	Air cooled	Cold water quenched
Silicate content, f_s (wt%)	0	0	1.7	1.7	3.7	3.7
Tensile modulus (GPa)	1.1	1.1	1.5	1.5	1.8	1.8
Tensile strength (MPa)	49.2	52.6	66.8	65.4	78.3	83.4
Ductility (%)	124	147	34	70	8	32
Fracture work (J)	1.11	1.02	0.64	0.98	0.22	0.72
Average spherulite size (μm)	83	5.9	27	5.3	18	6.4
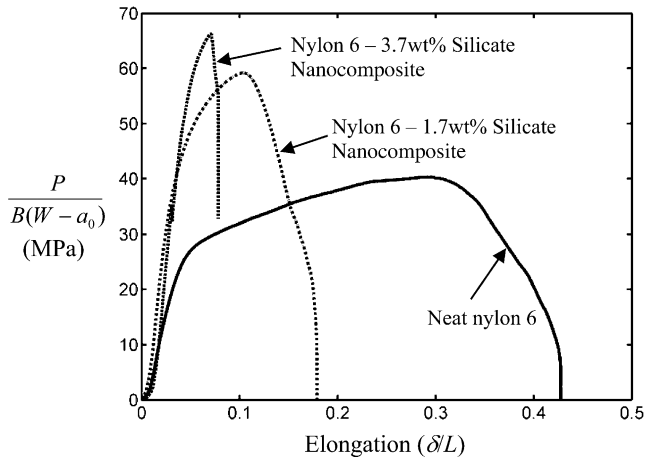
Fig. 2. The typical stress–strain curves of fracture experiment of the air cooled samples.

Fig. 4. The fracture work as function of the silicate content.

Figs. 2 and 3 show the typical stress–strain curves of the air cooled samples and cold water quenched samples, respectively, where P is the applied load and δ is the displacement. The total fracture work, W_f, is shown in Fig. 4.

2.3. Wide angle X-ray diffraction

The semi-crystalline structure of the samples were analyzed through wide-angle X-ray diffraction scanning (WXDS) using a 40 mA–40 kW Bruker AX8 diffractometer with Cu Kα_1 radiation. In order to minimize the size effect, the samples were thinned to less than 100 μm through mechanical polishing followed by a thorough rinsing in methanol. The scan speed was 1°/min. The results are shown in Figs. 5 and 6.

2.4. Polarized optical microscopy

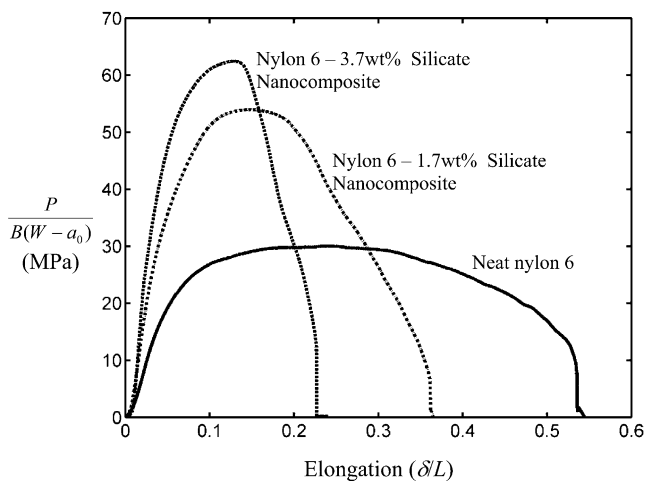In order to directly observe the spherulite structure, nanocomposite thin films were produced for the polarized

optical microscopy (POM) study. After drying, the pellets were hot pressed between two glass slides at 240 °C, and then either quenched in cold water or air cooled together with the steel mold used in the preparation of the fracture specimens, such that the cooling rate was about the same. The plate thickness was approximately 100 μm. Fig. 7 shows the microscopy of the air cooled samples, and Fig. 8 shows that of the quenched samples. The average spherulite sizes were calculated by a Matlab image processing program and the results are listed in Table 1. The standard deviations were about 30–40% of the mean values.

3. Discussion

The peak crystallization temperature of nylon polymers is around 150–200 °C [16,17]. For air cooled samples, since the materials stayed in this temperature range for a relatively long time, the semi-crystalline structure was quite coarse, as shown in Fig. 7(a). During the cold water quenching, however, the sample temperature was reduced from 240 °C

Fig. 3. The typical stress–strain curves of fracture experiment of the cold water quenched samples.

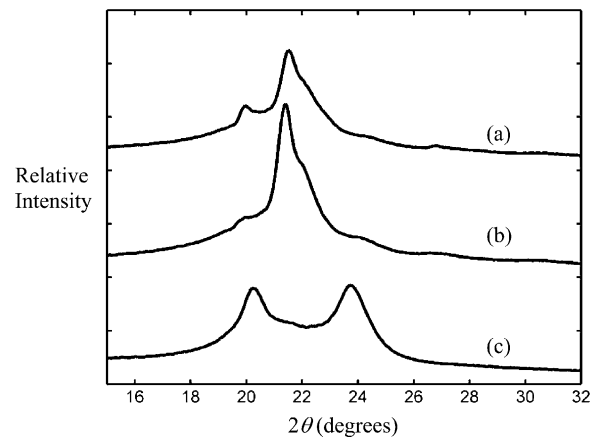Fig. 5. X-ray diffractometer scans for the air cooled nanocomposites with the silicate contents of (a) 3.7 wt%; (b) 1.7 wt%; and (c) 0 wt%.
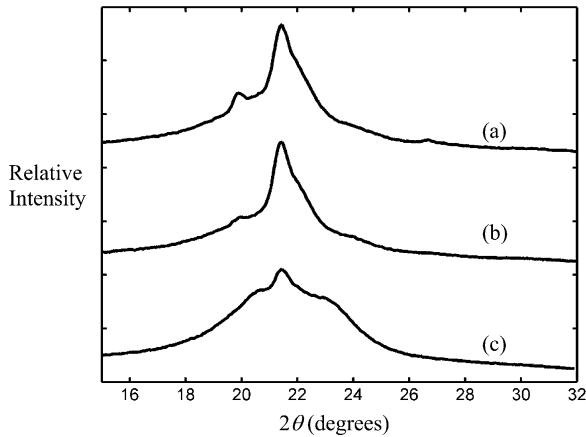
Fig. 6. X-ray diffractometer scans for the cold water quenched nanocomposites with the silicate contents of (a) 3.7 wt%; (b) 1.7 wt%; and (c) 0 wt%.

to room temperature in seconds. Under this condition, the non-isothermal nature of the crystallization must be taken into consideration. As the cooling rate increases, the crystallite growth is suppressed and thus the spherulite size is relatively small. The influences of processing conditions on the crystallization parameters have been discussed in detail by Xu et al. [11]. It has been reported by a number of research teams that in the melt-crystallized thermoplastic matrix, with increasing nanofiller content the crystallinity can be either reduced or increased slightly, or nearly constant, while the spherulite size is considerably decreased [6,7,18,19], as shown in both Figs. 7 and 8. This phenomenon was attributed to the promotion of nucleation by the nanofillers and the reduction in molecular mobility in the amorphous phase, which is compatible with the observation that the improvement in stiffness of nanocomposites is more significant at higher temperatures [19,20]. The comparison of Figs. 7 and 8 indicates that the influences of cooling rate and silicate nanolayers on the spherulite size are somewhat comparable to each other. The effect of nanofillers is quite pronounced when the cooling rate is low. In quenched samples, on the other hand, the average spherulite size is insensitive to the silicate content, f_s (see Table 1), probably because that the constraint of the nanofillers on the chain mobility has saturated. If the spherulite size is large, fracture tends to occur along
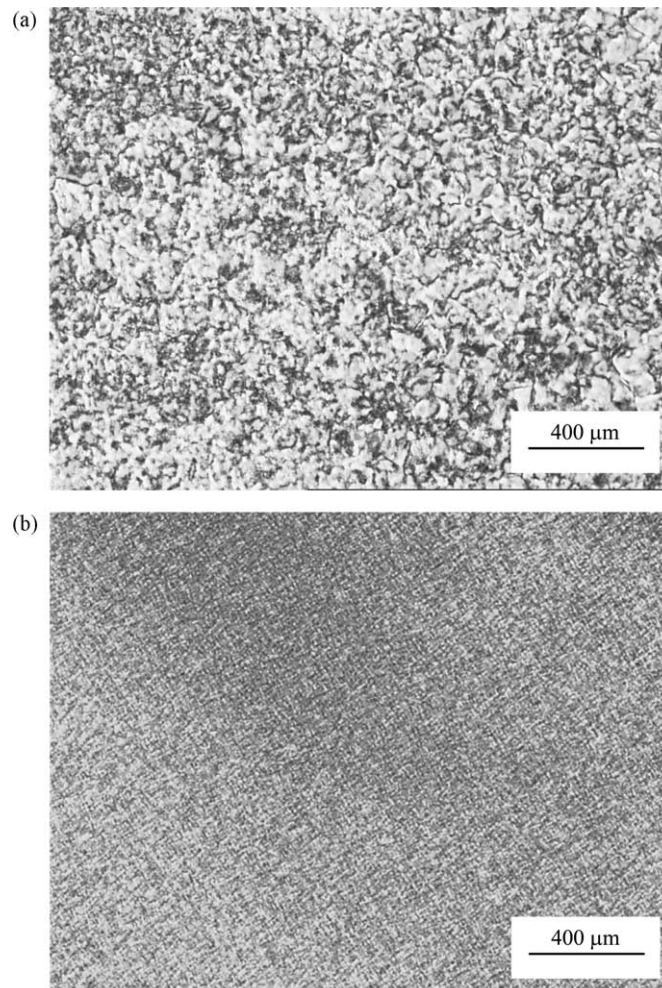

Fig. 7. Polarized optical microscopy of the neat nylon 6: (a) air cooled; (b) cold water quenched.
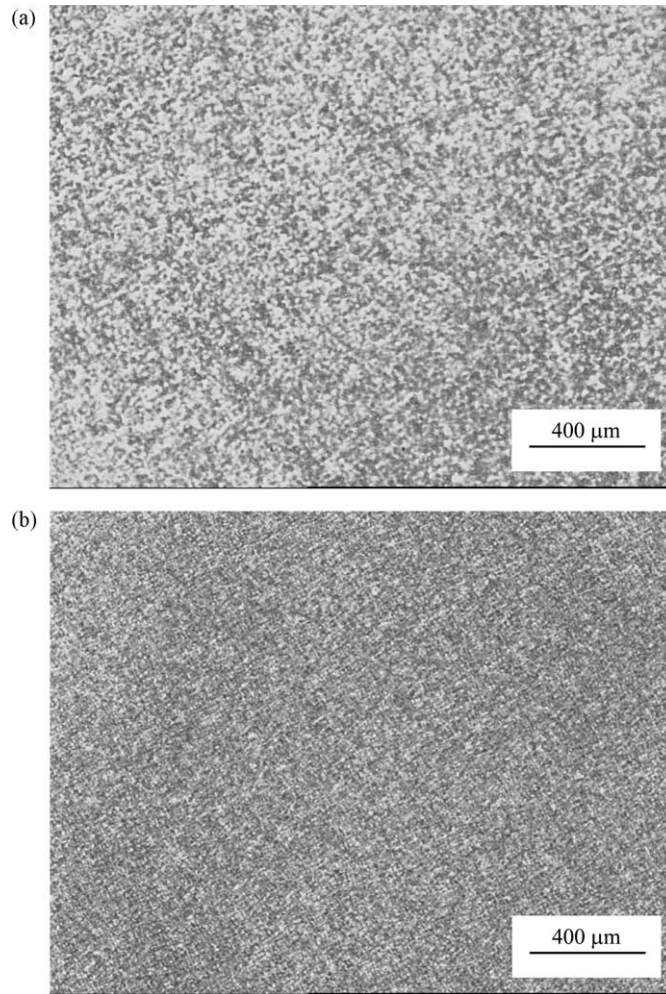
(a)

(b)

Fig. 8. Polarized optical microscopy of the nylon 6–3.7 wt% nanocomposite: (a) air cooled; (b) cold water quenched.

the relatively weak boundaries; if it is smaller than the characteristic microstructure length, the fracture behavior of the material resembles that of amorphous polymers [21]. Very often, as the spherulite size decreases the tie-molecule density will increase [22]. Thus, increasing cooling rate has a beneficial effect to the fracture resistance (see Figs. 2–4).

As the silicate content increases, the tensile moduli and strengths of both air cooled and cold water quenched samples become higher. This phenomenon is one of the major attractions of the nylon 6-silicate nanocomposites. However, the ductility tends to decrease with increasing f_s. Since the silicate nanolayers are much smaller than the crack tip plastic zone size, the ordinary reinforcing mechanisms such as crack trapping and bridging are negligible [23,24]. The nanolayers can act as stress concentrators and cause microvoiding around them, and it has been reported that it is difficult for the microvoids to grow into the matrix [25,26]. Furthermore, the local strengthening effect will suppress the breakdown of mosaic blocks, which is an important mechanism of craze initiation [22]. Consequently, as the silicate content increases, the ability to craze is reduced. By comparing Figs. 2–4, it can be

seen that for neat nylon 6 where the plastic flow is dominated by cold drawing, the fracture resistance is insensitive to the cooling rate. With the addition of the nanofillers, crazing becomes important [25,26] and W_f of the quenched samples is much higher. Actually the fracture resistance of quenched NS-17 is about the same as that of neat nylon, although when the silicate content increases to 3.7 wt% there are evidences showing that W_f starts to decrease with f_s. Because the variation in cooling rate has little influence on neat nylon 6, the effect of non-isothermal crystallization should be more important in crazing. Thus, the beneficial effect of increasing cooling rate on fracture toughness of nanocomposites should be attributed to either (1) with a high cooling rate the tie-molecule density is increased or (2) the craze initiation is easier, or both. These factors should mostly affect the number of crazes and the craze growth rate instead of the initiation condition of crazing, since, as shown in Table 1, the tensile strength is somewhat independent of the cooling rate.

In semi-crystalline nylon polymers there are two basic forms, α and γ [21]. The α form is characterized by the monoclinic unit cell with a zig–zag planar configuration,

which has two repeat distances of 0.44 and 0.37 nm. Correspondingly, the peak reflection occurs at $2\theta = 20.5°$ and 24°. The γ form consists of parallel chains with amide groups twisted from methylene group planes, where the repeat distance is 0.42 nm and the peak reflection 2θ angle is about 21.5° [10]. The crystallinity in both forms is insensitive to the addition of the nanofillers [14]. According to the WXDS results of aircooled samples shown in Fig. 5, in neat nylon the proportion of the α form is much higher than that of the γ form. In NS-17, however, the γ form becomes dominant and the contribution of the α form to the relative intensity is almost negligible. As the silicate content increases to 3.7 wt%, in NS-37, while the major part of the crystalline phase is still in the γ form, the content of the α form increases. This demonstrates clearly that the presence of nanofillers can promote the formation of the γ form, especially when f_s is relatively low, probably due to the self-organization of the crystallized macromolecules at the filler–matrix interface. It has been observed that in injection molded nylon 6-silicate nanocomposites the lamella can orient at the nanolayer surface with the hydrogen-bonded planes perpendicular to the axial direction [25]. If the silicate content is relatively high, the nanolayers tend to form a three-dimensional network and thus the crystallization process is more localized. According to Fig. 6, with increasing cooling rate, while in cold water quenched N-6 the content of the γ form is much higher than that in air cooled samples, as f_s increases the fractions of the α form are about the same. Therefore, the toughening effect of the addition of nanolayers should not be attributed to the variation in the α/γ ratio.

4. Conclusions

In this paper, the effect of cooling rate on toughness of nylon 6-silicate nanocomposites was studied through a set of fracture experiments. There exist at least two competing mechanisms that govern the failure behavior related to the matrix morphology change and the filler–matrix interaction, respectively. The fracture resistance, which is usually the weakest aspect of the nanocomposites, can be enhanced significantly by cold water quenching. The following conclusions are drawn:

(1) The influence of cooling rate on the tensile modulus and strength is negligible.
(2) The fracture resistance of neat nylon 6 is insensitive to the increase in cooling rate.
(3) With the addition of silicate nanolayers, increasing cooling rate has a beneficial effect to the fracture toughness.
(4) Both increasing cooling rate and addition of silicate nanolayers lead to finer semi-crystalline matrix structure.

References

[1] Kato M, Usuki A. Polymer–clay nanocomposites. In: Pinnavaia TJ, editor. Polymer–clay nanocomposites. New York: Wiley; 2000.
[2] Giannelis EP. Polymer layered silicate nanocomposites. Adv Mater 1996;8:29.
[3] Yasue K, Katahira S, Yoshikawa M, Fujimoto K. In situ polymorization route to nylon 6-clay nanocomposites. In: Pinnavaia TJ, Beall GW, editors. Polymer–clay nanocomposites. New York: Wiley; 2000.
[4] Krishnamoorti R, Giannelis EP. Rheology of end-tethered polymer layered silicate nanocomposites. Macromolecules 1997;30:4097.
[5] Masenelli-Varlot K, Erynaud E, Vigier G, Varlet J. Mechanical properties of clay-reinforced polyamide. J Polym Sci 2002;B40:272.
[6] Tjong SC, Meng YZ, Xu Y. Structure and properties of polyamide-6/vermiculite nanocomposites prepared by direct melt compounding. J Polym Sci 2002;B40:2860.
[7] Giza E, Ito H, Kikutani T, Okui N. Fiber structure formation in high-speed melt spinning of polyamide 6/clay hybrid nanocomposites. J macromol Sci Phys 2000;B39:545.
[8] Kojoma Y, Matsuoka T, Takahashi H, Kurauchi T. Crystallization of nylon 6-clay hybrid by annealing under elevated pressure. J Appl Polym Sci 1993;51:683.
[9] Wu TM, Liao CS. Polymorphism in nylon 6/clay nanocomposites. Macromol Chem Phys 2000;201:2820–5.
[10] Liu X, Wu Q. Nonisothermal crystallization behaviors of polyamide 6/clay nanocomposites. Eur Polym J 2002;38:1383–9.
[11] Xu W, Liang G, Wang W, Tang S, He P, Pan WP. Poly(propylene)-poly(propylene)-grafted maleic anhydride-organic montmorillonite (PP-PP-g-MAH-Org-MMT) nanocomposites. II. Nanoisothermal crystallization kinetics. J Appl Polym Sci 2003;88:3093–9.
[12] Hasegawa N, Okamoto H, Kato M, Usuki A, Sato N. Nylon 6/Na-montmorillonite nanocomposites prepared by compounding nylon 6 with Na-montmorillonite slurry. Polymers 2003;44:2933–7.
[13] Usuki A, Kojima Y, Kawasumi M, Okada A, Fukushima Y, Kurauchi T, Kamigaito O. Synthesis of nylon 6-clay hybrid. J Mater Res 1993;8:1179–84.
[14] Kojima Y, Usuki A, Kawasumi M, Okada A, Fukushima Y, Kurauchi T, Kamigaito O. Mechanical properties of nylon 6-clay hybrid. J Mater Res 1993;8:1185–9.
[15] Usuki A, Hasegawa N, Kadoura H, Okamoto T. Three dimensional observation of structure and morphology in nylon-6/clay nanocomposite. Nanoletters 2003;1:271–2.
[16] Rubinstein M, Colby RH. Polymer Physics. Oxford: Oxford University Press; 2003.
[17] Ozawa T. Kinetics of non-isothermal crystallization. Polymers 1971;12:150–8.
[18] Wang KH, Choi MH, Koo CM, Xu M, Chung IJ, Jang MC, Choi SW, Song HH. Morphology and physical properties of polyethylene/silicate nanocomposite prepared by melt intercalation. J Polym Sci 2002;B40:1454.
[19] Chan C, Wu J, Li J, Cheung Y. Polypropylene/calcium carbonate nanocomposites. Polymers 2002;43:2981.

[20] Krishnamoorti R, Giannelis EP. Rheology of end-tethered polymer layered silicate nanocomposites. Macromolecules 1997; 30:4097.

[21] Russell DP, Beaumont PWR. Structure and properties of injection-molded nylon 6 parts 1, 2, 3. J Mater Sci 1980;15:197.

[22] Kambour RP. A review of crazing and fracture in thermoplastics. Macromol Rev 1973;7:1.

[23] Qiao Y, Kong X. Unstable crack advance across a regular array of short fibers in brittle matrix. Compos Sci Technol 2004;64:711.

[24] Qiao Y. Fracture toughness of composite materials reinforced by debondable particulates. Scripta Mater 2003;49:491.

[25] Kim GM, Lee DH, Hoffmann B, Kressler J, Stoppelmann G. Influence of nanofillers on the deformation process in layered silicate/polyamide-12 nanocomposites. Polymers 2001;42:1095.

[26] Labour T, Vigier G, Seguela R, Gauthier C, Orange G, Bomal Y. Influence of the β-crystalline phase on the mechanical properties of unfilled and calcium carbonate-filled polypropylene: ductile cracking and impact behavior. J Polym Sci 2002;B40:31.